

Manuscript Number: SMM-18-2435R1

Title: High-temperature flexural strength performance of ternary high-entropy carbide consolidated via spark plasma sintering of TaC, ZrC and NbC

Article Type: Regular article

Keywords: tantalum carbide; high-entropy ceramics; flexural strength; high temperature materials.

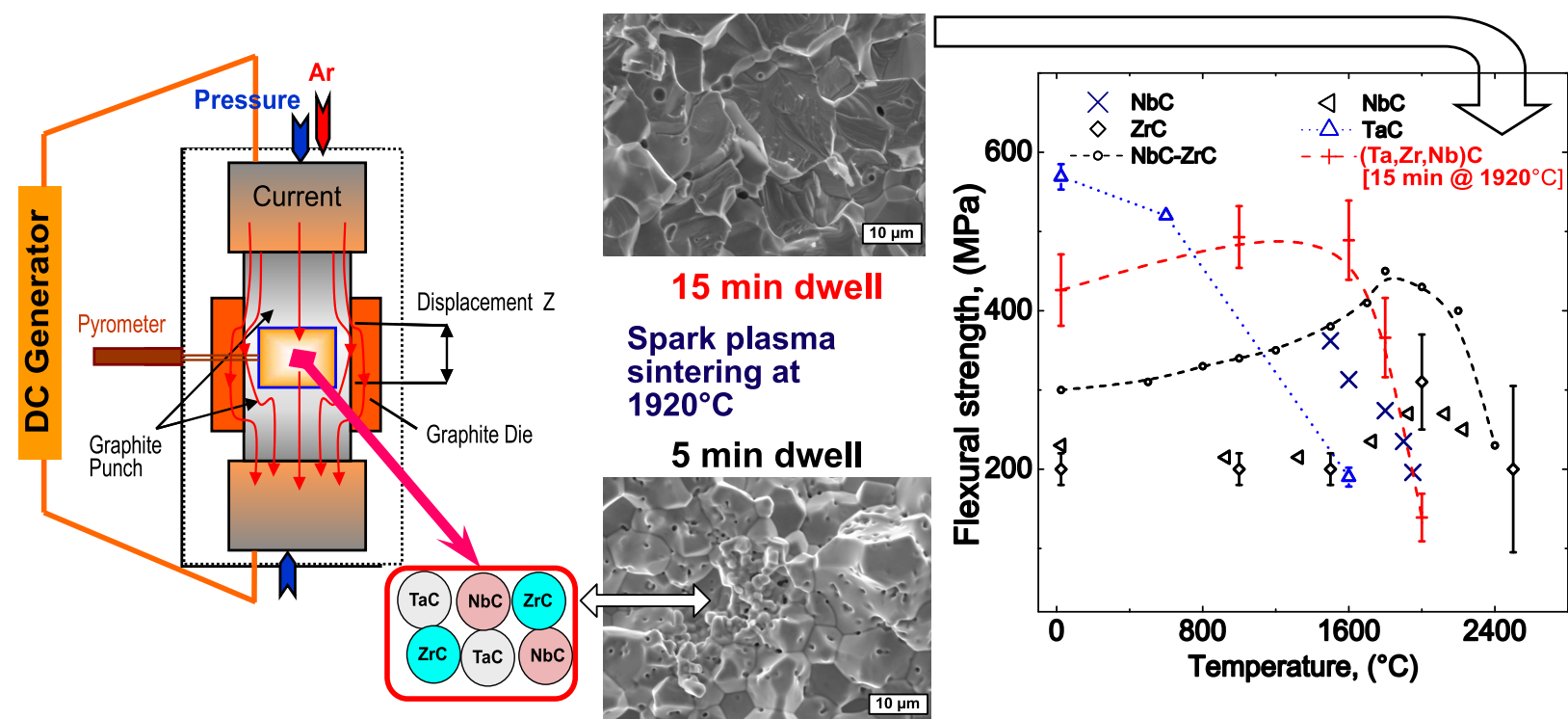
Corresponding Author: Dr. Dmytro Demirskyi, Ph.D.

Corresponding Author's Institution: Tohoku University Advanced Institute for Materials Research (AIMR)

First Author: Dmytro Demirskyi, Ph.D.

Order of Authors: Dmytro Demirskyi, Ph.D.; Hanna Borodianska; Tohru Suzuki; Yoshio Sakka; Kyosuke Yoshimi; Oleg Vasylykiv

Abstract: The solid solution formation and consolidation of the (Ta,Zr,Nb)C single-phase ceramic made from commercial TaC, ZrC and NbC powders prepared by spark plasma sintering at the temperature of 1920 °C was investigated. Phase analysis and lattice parameter measurements by X-ray diffraction showed multi-stage formation of the single-phase high-entropy-type carbide with the lattice parameter of 4.535 Å. The flexural strength and fracture toughness at room temperature were 460±24 MPa and 2.9 MPa m^{1/2}, respectively. With an increase in temperature, the flexural strength showed an increase up to 1600 °C to 496±44 MPa, then decreased after 1800 °C to 366±46 MPa.



Dear editor of the Scripta Materialia Prof. Nitin Padture,

We would like to submit the revised version manuscript entitled “High-temperature flexural strength performance of ternary high-entropy carbide consolidated via spark plasma sintering of TaC, ZrC and NbC” (SMM-18-2435) by Dmytro Demirskyi et al.

First, the authors would like to express our gratitude to you, and reviewer for an opportunity to present our latest findings in Scripta Materialia.

In the revised manuscript, changes were highlighted using a yellow background color.

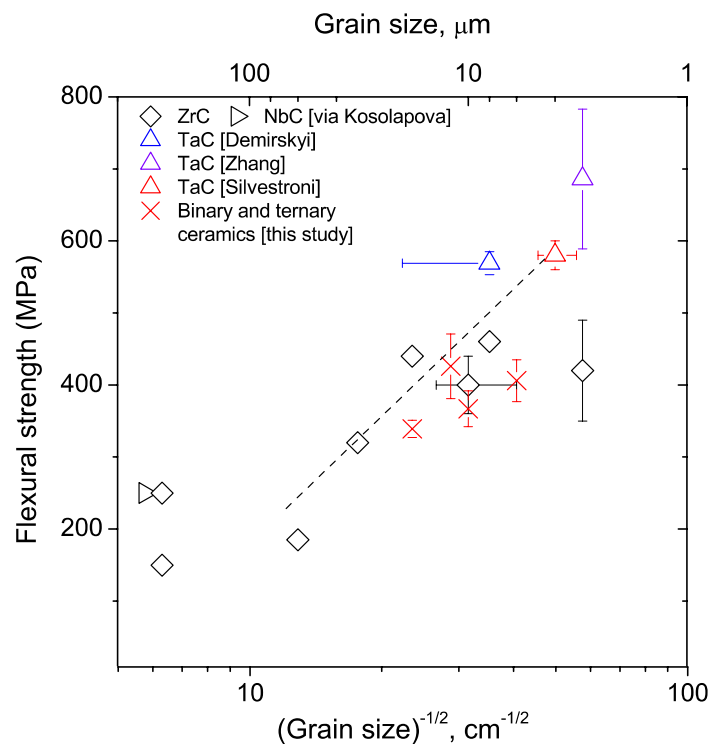
Please find below our concise answers to the reviewer comments:

1) Binary (Hf,Ta)C and high-entropy carbides exhibit higher hardness compared to the base monocarbides, suggesting a strengthening mechanism at room temperature reported recently by Smith et al. (C.J. Smith, Acta Mater 145 (2018) 142-153) and Castle et al. (ref [1]).

Regarding the flexural strength of carbides measured at RT, this seems to be in agreement with that was reported for (Nb,Zr)C compared to NbC and ZrC, as it was mentioned by the authors. What could be the reason of that this flexural strength enhancement is not valid for (TaNbZr)C and results in lower flexural strength compared to TaC? Does it mean different strengthening mechanisms at RT than that was reported by Castle et al., or could be attribute to the different microstructures (i.e. more pores in TZN than in TaC)?

The strengthening mechanisms proposed in these two works comforts hardness data for binary carbides, but in terms of the flexural behavior, at least two more factors may influence ceramics performance.

Firstly the flexural strength at the ambient temperature can be viewed as a function of grain size. The figure below provides such an analysis. One can see that tantalum carbide data have the highest flexural strength. These TaC bulks have 4-8 % of pores. Data for ZrC and NbC were selected for specimens with porosity less than 10%.



Effect of the grain size on the flexural strength of selected carbide bulks at room temperature

L. Silvestroni et al., 10.1016/j.compositesb.2014.11.043.

X. Zhang et al., 10.1016/j.msea.2008.09.024.

D. Demirskyi et al., 10.1016/j.ceramint.2015.09.065.

T. Ya Kosolapova (ed.), Properties, Preparation and Application of High-Melting Compounds: Reference Book, Metallurgiya, Moscow, 1986 (in Russian), references 485, 489, 550, 593.

One can see that tantalum carbide bulks have greater flexural strength when compared to ZrC or NbC, while the data for TZN and binary carbide systems

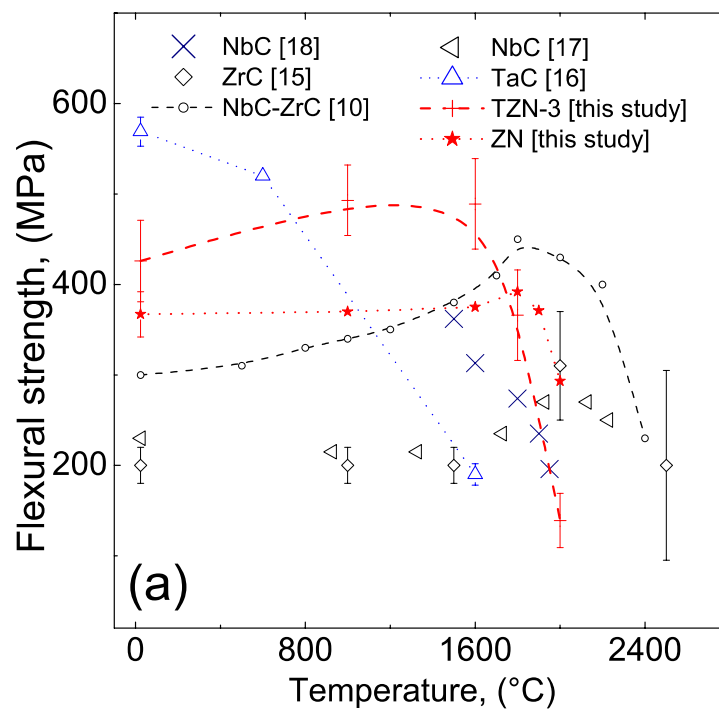
comport the Hall-Petch like relation. It seems to us that at this point the grain size can be considered as an adequate explanation for the TZN performance at room temperature when compared to TaC. Ultimately, we hoped to achieve the ~ 600 MPa at room temperature, and that is why the TaC was a key component in this ceramic. But grain growth and a different pore size distribution, perhaps, leads to the degradation of flexural strength. Perhaps if we can consolidate TZN ceramic with a grain size of below 5 μm it will be possible to flexural strength similar to TaC bulks.

Another possible explanation for RT data may lie in the stresses accumulated during processing. Our previous experience with NbB_2 (10.1111/jace.15048) [ref 11] suggests that if this explanation is correct TZN bulks may have higher strength at ambient temperature within 10% increase. But due to the time restriction, we will examine the flexural strength performance of the annealed SPSed specimens in the soonest case in Feb-Mar 2019.

2.)In addition to this, the peak position of strength and temperature of (Nb,Zr)C binary carbide shows a increment in comparison with NbC and ZrC but it's not valid for TZN. Please, comment on this.

This is, perhaps, the most important feature of the attempted analysis. Because the information of the flexural strength performance on (Ta,Zr)C and (Ta,Nb)C ceramics is unknown the explanation for the observed behavior can be argued as follows.

We attempted to verify the high-temperature flexural strength of ZN ceramic with only one sample for tests at 1000 °C, 1600 °C, 1800 °C, 1900 °C and 2000 °C. One can see that ZN data agrees with findings of [10] for (Zr,Nb)C, while the peak in strength was observed at 1800 °C.



At this point we suspect that the difference between ZN data and reported in [10] can be due to processing. Specimens in [10] were prepared by the pressureless sintering at above 2500 °K. Namely, the higher consolidation temperature may allow shifting the brittle to plastic transition temperature to higher values or to restrict some fracture mechanism such as grain-sliding [16]. As noted in the original draft, to confirm similar claims we need to investigate the behavior of TN and TZ ceramics. We anticipate that if the TN or TZ

somehow follows a trend of TaC reported in [16], the TZN behavior can be explained in terms of the effect of tantalum carbide. Other factors such as grain size and pore size may also cause a change in high-temperature fracture behavior.

Ideally, analysis for a ternary system should also include the preparation of the reference bulks (individual bulks and binary ceramics) with similar pore and grain size, hopefully, we can deliver such analysis for a different ternary carbide or boride system in the upcoming contributions.

3.)The scatter of flexural strength is missing at 1800 °C in the abstract.

Thank you, we revised abstract accordingly.

4.)The flexural strength - temperature plot should be increased in graphical abstract to be more visible (maybe by reorganizing SEM images).

Thank you, we reorganized the abstract so flexural strength behavior can be clearly viewed.

5.)Please, check the manuscript for spelling mistakes (e.g. r is missing in ZrC in the abstract).

Thank you, we asked an independent person to check the draft.

All authors have seen and approved the revised manuscript for submission to Scripta Materialia.

On behalf of authors,

Dmytro Demirskyi

High-temperature flexural strength performance of ternary high-entropy carbide consolidated via spark plasma sintering of TaC, ZrC and NbC

D. Demirskyi (a,b,c)†, H. Borodianska (b), T.S. Suzuki (b), Y. Sakka (b), K. Yoshimi (c), and O. Vasylykiv (b)†.

(a) National Institute for Materials Science, 1-2-1 Sengen, Tsukuba, Ibaraki 305-0047, Japan

(b) WPI-Advanced Institute for Materials Research (WPI-AIMR), Tohoku University, 2-1-1 Katahira, Aoba-ku, Sendai, 980-8577 Japan

(c) Department of Materials Science and Engineering, Tohoku University, 6-6-02 Aramaki Aza Aoba, Sendai, 980-8579, Japan

Abstract

The solid solution formation and consolidation of the (Ta,Zr,Nb)C single-phase ceramic made from commercial TaC, ZrC and NbC powders prepared by spark plasma sintering at the temperature of 1920 °C was investigated. Phase analysis and lattice parameter measurements by X-ray diffraction showed multi-stage formation of the single-phase high-entropy-type carbide with the lattice parameter of 4.535 Å. The flexural strength and fracture toughness at room temperature were 460±24 MPa and 2.9 MPa m^{1/2}, respectively. With an increase in temperature, the flexural strength showed an increase up to 1600 °C to 496±44 MPa, then decreased after 1800 °C to 366±46 MPa.

Keywords: tantalum carbide; high-entropy ceramics; flexural strength; high temperature materials.

Multicomponent carbides, the diborides of refractory metals, were recently synthesized or consolidated using various methods [1–6]. This interest in new ultra-high temperature

† Authors to whom correspondence should be addressed, Dmytro Demirskyi, demirskyi.dmytro.e2@tohoku.ac.jp /phone +81(0)70-2010-6281/ and Oleg Vasylykiv, oleg.vasylykiv@nims.go.jp /phone +81(0)80-4144-4747/

1 materials is caused by the ongoing search for a new class of ceramic materials capable of
2 withstanding high-temperatures, possess high modulus or ablation resistance. In [1], multi-
3 component carbides were synthesized by spark plasma sintering using the raw powders. A
4 single-phase ceramic with an enhanced nanohardness has been reported for the Hf-Ta-Zr-Nb-
5 C and Hf-Ta-Zr-Ti-C systems [1]. These were called high-entropy carbides, because similar
6 to high-entropy alloys [7], a single phase with an equimolar metal ratio was reported. Oxides
7 with similar features were also reported [8].

8
9
10
11
12
13
14
15
16
17 However, the hardness increase reported in [1], which is undoubtedly associated with lattice
18 strain due to the new solid-solution formation is not a novel phenomenon [9]. For the three-,
19 four- and five-component systems, the analysis of the properties can be quite complex [9], as
20 the contributions of processing route or individual phase to the hardness and modulus do not
21 follow the simple rule of mixtures. Furthermore, the majority of studies of high-entropy
22 carbides is expected such that ceramics may be considered as new high-temperature materials
23 [1,5,6].

24
25
26
27
28
29
30
31
32
33
34 Up to now, these expectations were not experimentally confirmed, hence, the present study
35 explores the high-temperature flexural strength behavior of the ternary TaC–ZrC–NbC
36 carbide system. The ultimate goal of this study is to synthesize/consolidate a single-phase
37 high-entropy carbide. However, more crucially, the study of the formation of this high-
38 entropy carbide ceramic by XRD was attempted. Thus three binary carbide systems were
39 synthesized. This step allowed us to identify the lattice parameter for the solid-solution and
40 also measure the flexural strength at room temperature. For the ternary TaC–ZrC–NbC
41 system, flexural strength at temperatures up to 2000 °C has been studied. The synthesized
42 high-entropy carbides were compared to the existing data for the (Zr,Nb)C [10] in order to
43 understand how to control or what to expect from the four- or five-component carbide
44 systems.

1
2
3
4
5
6
7
8
9
10
11
12
13
14
15
16
17
18
19
20
21
22
23
24
25
26
27
28
29
30
31
32
33
34
35
36
37
38
39
40
41
42
43
44
45
46
47
48
49
50
51
52
53
54
55
56
57
58
59
60
61
62
63
64
65

Commercially-available TaC, ZrC and NbC powders with the average powder particle size between 1 and 3 μm (Wako Pure Chemical Industries, Ltd., Osaka, Japan) were used as the starting materials. The major impurities in these carbides were O < 0.6 wt.%, Ti < 0.2 wt.% and Fe < 0.2 wt.%.

The as-received powders were mixed in an equimolar ratio, subjected to homogenization in alcohol, followed by drying at about 100 °C. The resultant powders were screened through 60 and 400 mesh screens. For simplicity, a ternary equimolar mixture was denoted as TZN, while the binary carbide solid-solid solutions were TZ, TN, and NZ (T for TaC, Z for ZrC and N for NbC, respectively). For the TZN ceramic, three different dwells were used at 1920 °C: TZN-1 (1 min), TZN-2 (5 min) and TZN-3 – 15 minute dwell.

The homogenized powder mixture was loaded into a graphite die with an inner diameter of 30 mm and subjected to the SPS. The outer surface of the die was wrapped in 5-mm-thick graphite felt to equilibrate the temperature distribution and reduce heat loss by radiation. The mold system containing the powder mixture was placed in an SPS furnace ('Dr. Sinter', SPS 1050, Sumitomo, Japan) [11]. The schedule for the TZN specimens prepared in this study had four major steps: (1) heating to 700 °C in four minutes following a five-minute dwell, (2) heating to 1400 °C in 10 minutes with a five-minute dwell; (3) five-minute ramp to 1920 °C, where dwells of 1, 5 and 15 minutes were used. The last step included a cooling down to 600 °C in 15 minutes. Steps (1) and (2) were performed in a vacuum; during the dwell at 1400 °C, the SPS chamber was backfilled with argon. At the end of the dwell at stage (2), the pressure was increased from 15 to 32 kN. The pressure of 32 kN was maintained during the consolidation and cooling stages as the application of lower pressures did not result in dense materials. Argon gas at the flow rate of 2 L/min was used.

The sintered specimens were ground using diamond disks with a particle size of up to 0.5 μm .

1 The three-point flexural strength was determined according Japanese Standard JIS R160
2 using rectangular bars (3×2×20 mm) cut from the specimens with a diameter of 30 mm by
3 electric discharge machining. Their lateral surfaces were ground and polished using diamond
4 pastes. The flexural strength tests were conducted at room temperature and at 1600 °C in
5 argon using a Shimadzu AG-X plus system (Shimadzu, Japan). Tests were performed using
6 semi-articulated fixtures according to ASTM Methods C1161-13 and C1211-13. The span of
7 16 mm and loading speed of 0.5 mm/min were used. Loading speed of 2 mm/min was used at
8 2000 °C. Eight bars were tested for each specimen at room temperature, and four specimens
9 at and above 1600 °C. The heating procedure for the high-temperature flexure tests at
10 1800 °C and 2000 °C are described in detail elsewhere [11,12].
11
12
13
14
15
16
17
18
19
20
21
22
23

24 The fracture toughness of the composites was evaluated using specimen testing in bending
25 which contained a single edge through-thickness notch in accordance with ASTM C1421–10.
26
27
28
29 Eight tests were conducted at room temperature.
30

31 The density of the samples was then measured by Archimedes method using ethanol as the
32 medium in accordance with ASTM B 963–08.
33
34
35

36 Microstructural observations and analyses were carried out on the fractured surfaces using a
37 scanning electron microscope (SEM, JCM-6000, JEOL). Observations were made on the
38 fractured surfaces after the flexural tests.
39
40
41
42

43 An X-ray diffraction (XRD) analysis (D8 Advance, Bruker, Karlsruhe, Germany) was
44 performed on the polished surfaces of the bars before the flexural tests in order to identify the
45 crystalline phases using the Cu-K α radiation.
46
47
48
49
50

51 The bulk density of the SPSed TZN ceramics are 9.22 g/cm³ (15 min dwell), 9.11 g/cm³ (5
52 min dwell) and 8.58 g/cm³ using a one-minute dwell at 1920 °C. Based on the X-ray
53 diffraction analyses (**Fig. 1**), after the SPS consolidation at 1920 °C and a dwell of 15
54 minutes, a single-phase ceramic was formed. Only for mirror polished specimens using a
55
56
57
58
59
60
61
62
63
64
65

1 logarithmic vertical scale, some traces of an oxycarbide phase [13] near 33 °C in two theta
2 were noticed (**Fig. 1 (c)**).
3

4 **Figure 1 (b)** shows peaks corresponding to the (111) and (200) planes of the monolithic
5 carbides, binary TZ, TN and ZN carbides and the TZN consolidated at 1920 °C. **Figure 1 (c)**
6 shows the effect of the consolidation conditions on the evolution of the (111) peak; one can
7 see that the ceramics consolidated using a shorter dwell time of 1 or 5 minutes at 1920 °C had
8 essentially two binary solid solutions (close to equimolar NZ and NT) and some traces of a
9 ternary TZN solid-solution. The TZ solid-solid solution prepared as a reference in this study
10 had a high similarity to the TN phase presented in **Fig. 1**.
11

12 The lattice parameter of the ternary TZN phase in Fig. 1 (a) was estimated to be 4.535 Å. An
13 error of 0.001 Å was evaluated by Jade 8 (Materials Data, Inc., Livermore, CA, USA) during
14 the Rietveld refinement procedure. Thus a theoretical density of the TZN bulk was assumed
15 to be 9.52 g/cm³ from the XRD data assuming the equiatomic contribution of 1/3 of the Ta,
16 Zr and Nb atoms in the sodium chloride-type unit cell (i.e., four atoms for carbon and four
17 atoms for metal). The binary solid-solution had the following lattice parameters (with an
18 error of 0.002 Å): TN – 4.447 Å, TZ – 4.523 Å and NZ – 4.581 Å.
19

20 **Figure 1** shows that at the relatively low temperature of 1920 °C by changing the dwell time,
21 one can see a mixture of three individual carbides forms two binary carbide solid-solutions
22 close to the TN and NZ, and a ternary solid-solution (with lattice parameter of close to
23 4.527 Å). One can presume that due to the pulsed electrical current and applied pressure, the
24 formation of the TZN phase can be observed at lower temperatures than in [1,5,6], but
25 because most refractory carbides are essentially difficult to consolidate as bulk ceramics, the
26 relative density after SPS for 1 min at 1920 °C was approximately 90% of the theoretical
27 density. An increase in the dwell time to five minutes at 1920 °C achieved a density of 95%,
28 but the binary carbide solid-solid solutions were still detectable by XRD.
29
30
31
32
33
34
35
36
37
38
39
40
41
42
43
44
45
46
47
48
49
50
51
52
53
54
55
56
57
58
59
60
61
62
63
64
65

1
2
3
4
5
6
7
8
9
10
11
12
13
14
15
16
17
18
19
20
21
22
23
24
25
26
27
28
29
30
31
32
33
34
35
36
37
38
39
40
41
42
43
44
45
46
47
48
49
50
51
52
53
54
55
56
57
58
59
60
61
62
63
64
65

Only after a 15-minute dwell at 1920 °C, a single phase solid solution free of the binary TZ or NZ phases was obtained. An explanation of the multistage formation of the TZN solid solution would be based on the different diffusivity of the transition metal atoms in the binary carbide rock salt structure. An analogous suggestion was made in [1], but within the present study, it may be assumed that the Zr atoms were the fastest moving metal species [14].

The fracture at room temperature and elevated temperatures (**Fig. 2**) showed that in addition to a major TZN phase (96 vol.% by ImageJ), at least 2 vol.% of the zirconium-rich oxycarbide phase (C to O 74:16 wt.% by EDX) was detected. Similar to the findings of [8], formation of the high-entropy oxycarbide is possible, as the Ta and Nb ions were detected by EDX in negligible quantities to Zr, i.e., 2/9 and 2/25, respectively. This phase was most likely formed during cooling, as it was usually located at grain boundaries and its triple-junctions. Zirconium carbide is known to be capable of containing a considerable amount of oxygen without altering the cubic lattice [13]. Furthermore, this oxycarbide phase was present in the vicinity of the gas entrapped pores. This phase is marked by the white arrows in **Fig. 2**, and the lattice parameter evaluated using weak peaks shown in **Fig. 1** was 4.68 Å, which is in reasonable agreement with the data of [13] for zirconium oxycarbide.

Another observation made for the microstructure is that microcracks were observed in all the specimens, even after quasi-plastic fracture at 1600 °C. It is thought that this may be a *special feature* of these compounds as quite large thermal stresses and lattice strains are expected to be present after the high-temperature consolidation.

In terms of the homogeneity of the grains, one can see that an almost equiatomic composition was observed for the individual grains (inset in **Fig. 2** shows the EDX summary for the area marked in **Fig. 2 (c)**). Similar to the XRD, EDX mapping of the TZN-2 specimen showed a slight offset from the equiatomic ratio (**Fig. 2 (g)**). Fractography of this bulk obtained at elevated temperature showed that in some instances, grains with a size identical to the raw

1 particles were noticed. Along with an increased number of pores, these observations
2 suggested that SPS at 1920 °C with a 15-minute dwell was required to produce the single-
3 phase bulk ceramic.
4

5
6
7 Furthermore, in refs. [1,4], it was suggested that stresses associated with solid-solution
8 hardening during the synthesis of high-entropy carbides (*high-entropy alloy is a solid-*
9 *solution after all*) may result in a hardness increase. **Similar findings were reported recently**
10 **by Smith et al. for the binary TaC–HfC system [15].** It was also pointed out in ref. [1], that if
11 solid-solution strengthening plays significant role in high-entropy carbides their hardness or
12 yield stress will show a strong *temperature dependence*. Similar to the findings of [10], high-
13 entropy carbides may have a shift in the brittle to ductile transition temperature.
14
15
16
17
18
19
20
21
22
23

24 Up to now, other mechanical properties of high-entropy carbides such as flexural or
25 compressive strength, are still not reported. Which is surprising, as a key feature of the high-
26 entropy metallic alloys is the increased tensile strength over a wide temperature range [7].
27 Hence, the main question formulated this study is *will high-entropy carbides have a better*
28 *high-temperature performance?*
29
30
31
32
33
34
35

36 If the expectations of ref [1] are correct in respect to solid-solution strengthening of Hf-Ta-
37 Zr-Nb-C, the temperature dependence of the peak strength observed during the flexural
38 strength tests of high-entropy carbide should behave similarly to other binary solid-solution
39 systems. **Figure 3** summarizes available data on the flexural strength of monolithic carbides
40 [16–19] and NbC–ZrC solid-solution [10].
41
42
43
44
45
46
47

48 **Figure 3** shows that TZN-3 had a strength of 489±49 MPa at 1600 °C, but at 1800 °C and
49 2000 °C, the strength decreased to 366±46 MPa and 139±32 MPa, respectively. This may be
50 considered as a promising result, as previous study of the bulk TaC showed a strength of
51 200 MPa at 1600 °C [17]. Loading curves indicated a steep decrease in the elastic modulus at
52 tests of 1800 °C and 2000 °C. One can also see a color tone difference above and below
53
54
55
56
57
58
59
60
61
62
63
64
65

1
2
3
4
5
6
7
8
9
10
11
12
13
14
15
16
17
18
19
20
21
22
23
24
25
26
27
28
29
30
31
32
33
34
35
36
37
38
39
40
41
42
43
44
45
46
47
48
49
50
51
52
53
54
55
56
57
58
59
60
61
62
63
64
65

1600 °C, and the mixed fracture behavior of the TZN phase below 1600 °C. At 1800 °C and 2000 °C, predominantly transgranular fracture was observed, although roughly 10% of the grains fractured in an intergranular manner. TZN-1 and TZN-2 showed slightly inferior strengths at 1600 °C: 263 and 303 MPa, respectively. This can be attributed to the higher porosity of these bulks (compare **Figs. 2 (c and f)**).

For the present study at room temperature, among the binary carbides, specimen TN showed a highest strength, presumably due to the lowest grain size and acceptable level of porosity (~5%). In the respect to the flexural strength dependence binary ceramics comfort the Hall-Petch like relation. Despite the apparent porosity of 8% for the TaC ceramic specimens reported in [17], this ceramic exhibited the highest strength among data in **Fig. 3**. Other data on TaC bulks in [20,21] also report flexural strength above 580 MPa at the room-temperature. When compared to TaC, an inferior strength of TZN bulks may lie in the thermal stresses accumulated during processing, similar to findings in [11], and higher strengths are anticipated in the case of an optimized SPS processing [1].

The toughness of $2.9 \pm 0.3 \text{ MPa m}^{1/2}$ and elastic modulus of $563 \pm 19 \text{ GPa}$ were evaluated using three-point flexure tests at ambient temperature. These values are comparable to that reported for the individual carbides and high-entropy carbides [22]. One can presume that a strength increase observed up to 1600 °C can also be accompanied by the *unchanged* fracture toughness, as similar fracture mechanisms were observed in this temperature range, but such tests are anticipated to be carried out in the future. At ambient temperature, the toughness values agree favorably with the available data of the monolithic carbides [22].

In terms of the flexural strength, the results of [10] for NbC–ZrC binary solid-solution system showed a similar dependence to that observed in the present study, i.e. gradual increase in flexural strength with an increase in temperature. This similarity underline that governing role of the solid-solution strengthening in respect to flexural strength behavior of single-

1 phase high-entropy TaZrNb carbide. The only visible difference between TZN and NbC–ZrC
2 is that according to [10], a brittle to ductile transition temperature or temperature of activation
3 of the macroscopic plastic deformation was approximately evaluated as 2300 °K. After this
4 temperature, similar to the finding of the present study at 1800 °C and 2000 °C, a rapid
5 strength decrease was reported. Compared to the data of ZrC in [10] (not shown for clarity in
6 **Fig. 3**), the formation of a solid solution between NbC and ZrC allows a shift in the
7 characteristic from 1700 °C for the bulk ZrC (porosity of 6 %). The data for the bulk NbC
8 [18] show a local peak in strength at around 2050 °C. In this case, one should also consider
9 some possible effects of the porosity (10% in [18] for NbC) or grain size. **The position of the**
10 **peak strength for the TZN ceramic at 1600 °C is unclear right now, as data for elevated**
11 **fracture of TN and TZ were not previously reported. Thus it is not possible to speculate if**
12 **high-entropy carbides with TaC should follow a trend reported in [17] for tantalum carbide.**
13 **As a possible explanation one may notice that TZN and ZrC–NbC specimens in [10] were**
14 **produced using different methods. Specimens in [10] that is by pressureless sintering at**
15 **above 2500 °K [14], as result grain size and pore volume were different when compared to**
16 **TZN.**

17 The high-temperature strength dependence well agrees with the data of Kelly and Rowcliffe
18 for NbC [18], and at the same time, with the solid-solution data for ZrC–NbC [10]. Hence,
19 one can see that the formation of a complex solid solution allows manipulating the flexural
20 strength of the ternary, and hopefully, four-phase and five-phase high-entropy carbides, but at
21 the same time, there is the possibility that a binary solid-solution may have a better
22 performance at elevated temperature. An in-depth analysis of the high-temperature
23 performance of binary and higher component systems is considered as a priority in upcoming
24 research in order to clarify the flexural performance observed in the present study.

1
2
3
4
5
6
7
8
9
10
11
12
13
14
15
16
17
18
19
20
21
22
23
24
25
26
27
28
29
30
31
32
33
34
35
36
37
38
39
40
41
42
43
44
45
46
47
48
49
50
51
52
53
54
55
56
57
58
59
60
61
62
63
64
65

In summary, a ternary single-phase high-entropy TaZrNb carbide was obtained by spark plasma sintering at the temperature of 1920 °C. Phase analysis by X-ray diffraction showed the existence of an intermediate stage during the formation of the ternary solid-solution. This is expected to be also true for other multicomponent high-entropy carbides, as metal atoms have a different diffusivity in the newly formed phases. The flexural strength of the TaZrNb carbide showed a peak in its strength at 1600 °C to 496±44 MPa. Above this temperature, the carbide phase fractured in a different manner and was accompanied by a decrease in its strength and elastic modulus. Despite the contribution of plasticity to the fracture, a significant number of microcracks was observed for the specimen fractured at 1800 °C.

D.D. was supported by World Premier International Research Center Initiative (WPI), MEXT, Japan.

[1] E. Castle, T. Csanadi, S. Grasso, J. Dusza, M. Reece, *Sci. Rep.* 8 (2018) 8609.

[2] J. Gild, Y. Zhang, T. Harrington, S. Jiang, T. Hu, M.C. Quinn, W.M. Mellor, N. Zhou, K. Vecchio, J. Luo, *Sci. Rep.* 6 (2016) 37946.

[3] A. Vladescu, I. Titorencu, Y. Dekhyar, V. Jinga, V. Pruna, M. Balaceanu, M. Dinu, L. Pana, V. Vendina, M. Braic, *PLoS ONE* 11 (2016), Article E0161151.

[4] V.F. Gorban, A.A. Andreyev, G.N. Kartmazov, A.M. Chikryzhov, M.V. Karpets, A.V. Dolomanov, A.A. Ostroverkh, E.V. Kantsyr, *J. Superhard Mater.* 39 (2017) 166–171.

[5] J. Zhou, J. Zhang, F. Zhang, B. Niu, L. Lei, W. Wang, *Ceram. Int.* 44 (2018) 22014–22018.

[6] X.L. Yan, L. Contantin, Y.F. Lu, J.F. Silvain, M. Nastasi, B. Cui, *J. Am. Ceram. Soc.* 101 (2018) 4486–4491.

[7] E.J. Pickering, N.G. Jones, *Int. Mater. Rev.* 61 (2016) 183–202.

- 1
2
3
4
5
6
7
8
9
10
11
12
13
14
15
16
17
18
19
20
21
22
23
24
25
26
27
28
29
30
31
32
33
34
35
36
37
38
39
40
41
42
43
44
45
46
47
48
49
50
51
52
53
54
55
56
57
58
59
60
61
62
63
64
65
- [8] C.M. Rost, E. Sachet, T. Borman, A. Moballeggh, E.C. Dickey, D. Hou, J.L. Jones, S. Curtarolo, J.-P. Maria, *Nat. Commun.* 6 (2015) 8485.
- [9] P. Schwarzkopf, R. Kieffer, *Refractory Hard Metals: Borides, Carbides, Nitrides, and Silicides*, Macmillan, New York, 1953.
- [10] A.G. Lanin, P.V. Zubarev, K.P. Vlasov, *Atomic Energy* 74 (1) (1993) 40–44.
- [11] D. Demirskyi, I. Solodkyi, T. Nishimura, Y. Sakka, O. Vasylykiv, *J. Am. Ceram. Soc.* 100 [11] (2017) 5295–5305.
- [12] D. Demirskyi, O. Vasylykiv, *Mater. Sci. Eng. A.* 697 (2017) 71–78.
- [13] S.K. Sarkar, A.D. Miller, J.I. Mueller, *J. Am. Ceram. Soc.* 55[12] (1972) 628–630.
- [14] P.V. Zubarev, *High-temperature strength of the interstitial phases*, Metallurgiya, Moscow, 1985. (in Russian)
- [15] C.J. Smith, X.-X. Yu, Q. Guo, C.R. Weinberger, G.B. Thompson, *Acta Mater.* 145 (2018) 142–153.
- [16] R.A. Andrievski, I.I. Spivak, *Strength of Refractory Compounds*, Metallurgiya, Chelyabinsk, 1989. (in Russian), reference 542.
- [17] D. Demirskyi, T. Nishimura, Y. Sakka, O. Vasylykiv, *Ceram. Int.* 42 (2016) 1298–1306.
- [18] S.S. Ordan'yan, E.K. Stepanenko, I.V. Sokolov, *Izv. Vyssh. Uchebn. Zaved., Khim. Khim T.* 27[10] (1984) 1201–1203.
- [19] A. Kelly, D.J. Rowcliffe *J. Am. Ceram. Soc.* 50 (1967) 253–256.
- [20] L. Silvestroni, L. Pienti, S. Guicciardi, D. Sciti, *Compos. Part B: Eng.* 72 (2015) 10–20.
- [21] X. Zhang, G.E. Hilmas, W.G. Fahrenholtz, *Mater. Sci. Eng. A.* 501 (2009) 37–43.
- [22] B. Ye, Y. Chu, K. Huang, D. Liu, *J. Am. Ceram. Soc.*, 10.1111/jace.16141.

Figure Captions

Fig. 1. XRD patterns for TZN ceramic after spark plasma consolidation at 1920 °C for 15 min (#TZN-3 (red line)). TZN-1 and TZN-2 schedules in (c) were 1 min and 5 min dwell at 1920 °C, respectively. A single phase with lattice parameter of 4.535 Å was evaluated using Jade 8 (Materials Data, Inc., Livermore, CA, USA) following the Rietveld refinement procedure. Data in (c) are presented in a logarithmic scale.

Fig. 2. The microstructure of the #TZN-3 specimen after flexural strength tests at (a) room temperature, (b) 1000 °C, (c) 1600 °C, (d) 1800 °C, and (e) 2000 °C. The white arrows show the presence of microcracks, while the black arrows show the distribution of the zirconium-rich oxycarbide phase. The typical pore size for this specimen was ~ 0.5–1 µm. (f) shows the 1600 °C fracture of the #TZN-2, while (g) shows a metal distribution map for (f) following a quantitative analysis. In the center of (f), one can see the fracture of grains with a size identical to the initial particle size of powder used for consolidation, hence, the broad distribution count for the Me atoms in (g).

Fig. 3. Effect of temperature on the flexural strength of individual transition metal carbides and TZN ceramic. Argon was used during the high-temperature flexural strength tests for all the reported data. The data by Kelly and Rowcliffe [19] was measured using a four-point setup. (b) shows typical loading diagrams of the TZN ceramic tested at room temperature and at elevated temperatures by the three-point flexural strength test. (c) illustrates the effect of the composition on flexural strength at room temperature. The numbers correspond to the mean grain size.

Figure 1

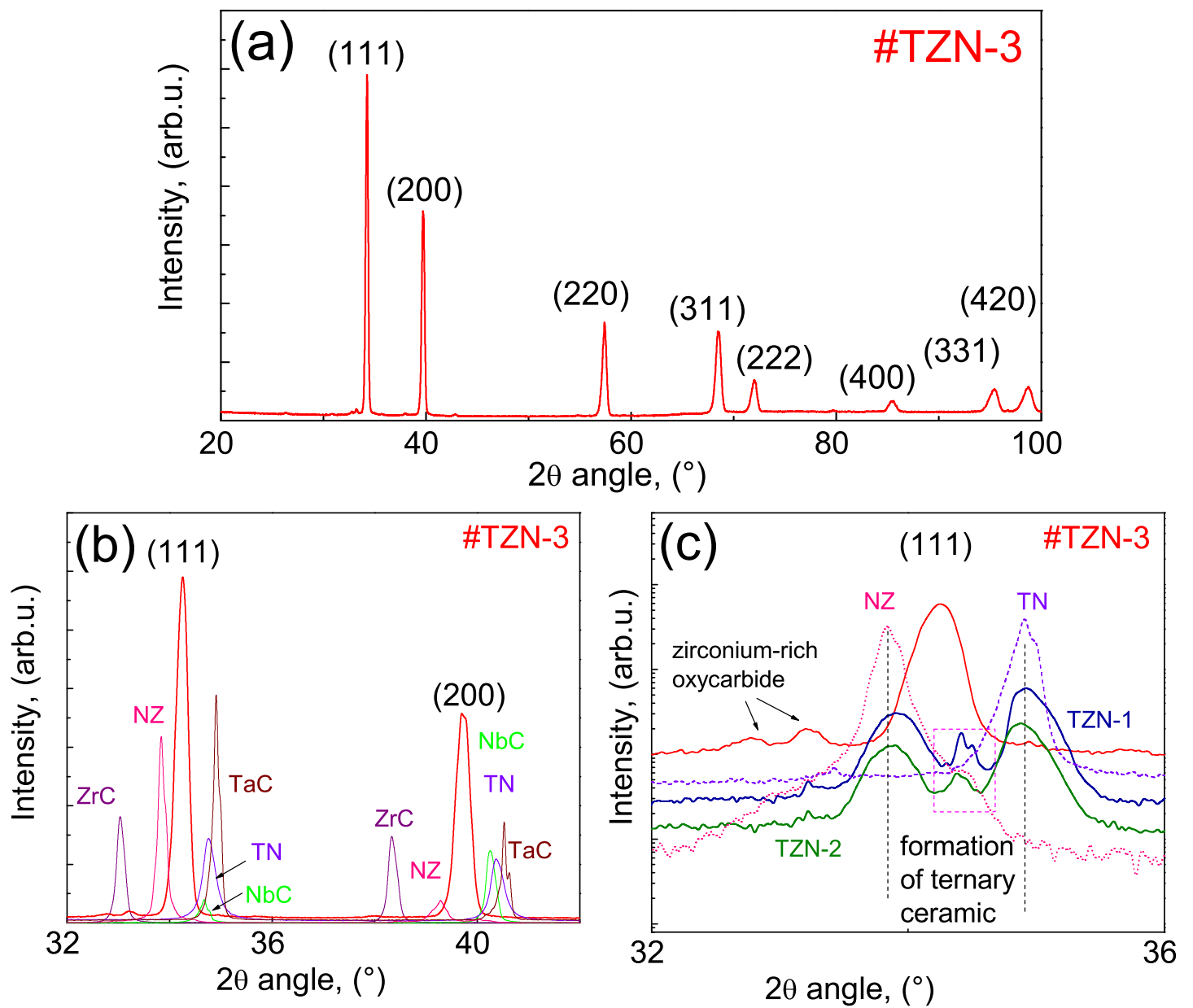


Figure 2
[Click here to download high resolution image](#)

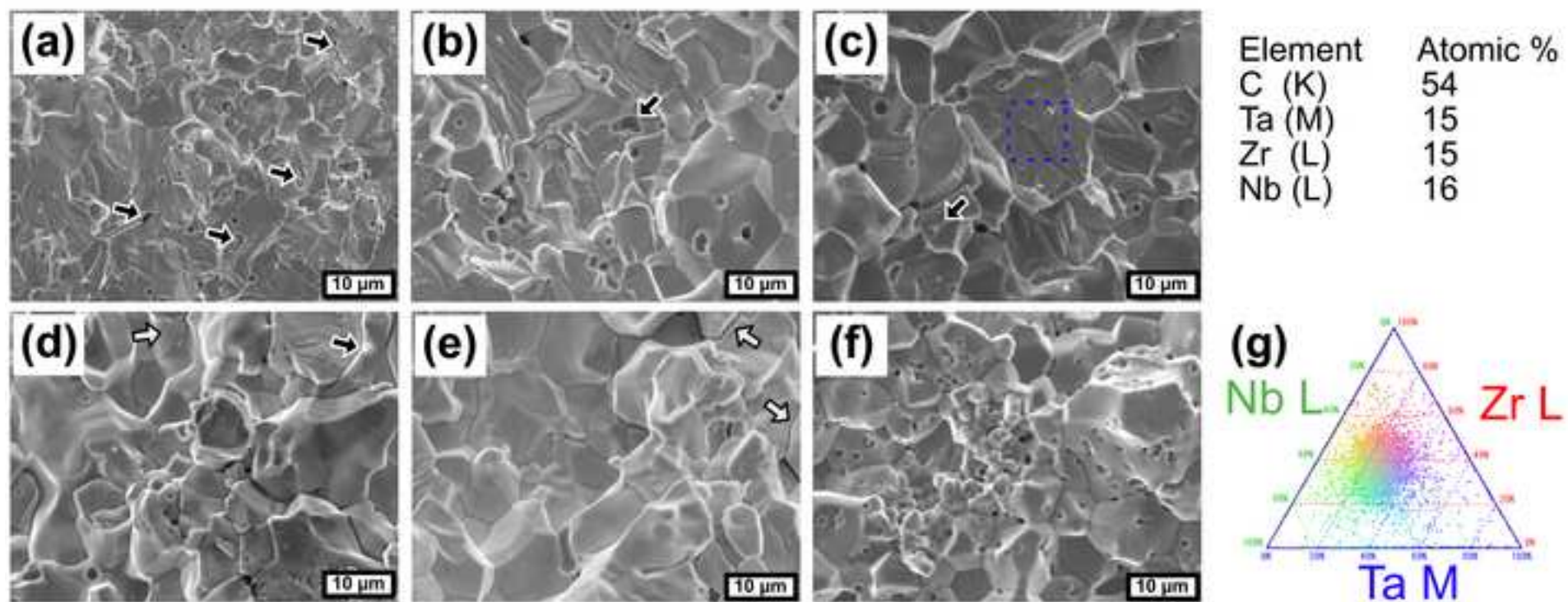


Figure 3

